HHS Public Access

Author manuscript

*Ann Biomed Eng*. Author manuscript; available in PMC 2024 August 28.

Published in final edited form as:

*Ann Biomed Eng*. 2024 August ; 52(8): 2013–2023. doi:10.1007/s10439-024-03495-z.

# A Data-Driven Approach to Estimate Human Center of Mass State During Perturbed Locomotion Using Simulated Wearable Sensors

**Jennifer K. Leestma**[1,2], **Courtney R. Smith**[3], **Gregory S. Sawicki**[1,2,4], **Aaron J. Young**[1,2]

[1]George W. Woodruff School of Mechanical Engineering, Georgia Institute of Technology, Atlanta, GA 30332, USA

[2]Institute for Robotics and Intelligent Machines, Georgia Institute of Technology, Atlanta, GA 30332, USA

[3]Wallace H. Coulter Department of Biomedical Engineering, Georgia Institute of Technology, Atlanta, GA 30332, USA

[4]School of Biological Sciences, Georgia Institute of Technology, Atlanta, GA 30332, USA

## Abstract

Center of mass (COM) state, specifically in a local reference frame (i.e., relative to center of pressure), is an important variable for controlling and quantifying bipedal locomotion. However, this metric is not easily attainable in real time during human locomotion experiments. This information could be valuable when controlling wearable robotic exoskeletons, specifically for stability augmentation where knowledge of COM state could enable step placement planners similar to bipedal robots. Here, we explored the ability of simulated wearable sensor-driven models to rapidly estimate COM state during steady state and perturbed walking, spanning delayed estimates (i.e., estimating past state) to anticipated estimates (i.e., estimating future state). We used various simulated inertial measurement unit (IMU) sensor configurations typically found on lower limb exoskeletons and a temporal convolutional network (TCN) model throughout this analysis. We found comparable COM estimation capabilities across hip, knee, and ankle exoskeleton sensor configurations, where device type did not significantly influence error. We also found that anticipating COM state during perturbations induced a significant increase in error proportional to anticipation time. Delaying COM state estimates significantly increased accuracy for velocity estimates but not position estimates. All tested conditions resulted in models with $R^2 > 0.85$, with a majority resulting in $R^2 > 0.95$, emphasizing the viability of this approach. Broadly, this preliminary work using simulated IMUs supports the efficacy of wearable sensor-driven deep learning approaches to provide real-time COM state estimates for lower limb exoskeleton control or other wearable sensor-based applications, such as mobile data collection or use in real-time biofeedback.

✉Jennifer K. Leestma, jleestma@gatech.edu.

**Competing Interests** The authors have no financial or non-financial interests to disclose.

**Keywords**

Center of mass state; Human intent recognition; Exoskeletons; Machine learning; Locomotion

## Introduction

Center of mass (COM) state is central to quantifying and controlling bipedal locomotion, where it is frequently used to inform step placement and quantify stability [1–3]. Bipedal robots benefit from knowledge of joint kinematics and segment properties, enabling accurate, real-time quantification of COM mechanics relative to the ground contact point. However, this is not so easily achievable in humans, where knowledge of participant-specific segment properties is unknown and joint encoders or goniometers are not necessarily available during biomechanics or wearable robotic experiments to provide lower limb kinematics. Previous studies have investigated wearable sensor-based methods for global COM state estimation, providing information such as walking speed and direction [4]. However, estimating COM state in a local frame, relative to the center of pressure (COP), would be more influential for understanding biomechanical stability by indicating COM mechanics relative to the ground contact point. Thus, real-time estimation of a human's COM state in a local frame could inform new approaches for wearable robotic exoskeleton control architectures, or other use cases such as mobile data collection or real-time biofeedback.

Specifically, knowledge of COM state during perturbed locomotion could enable the autonomous deployment of stability-augmenting wearable robots. Previous studies in this area have used COM state to detect environmental perturbations and inform exoskeleton assistance profiles, but have relied on simple models or motion capture to quantify COM mechanics, which confines use cases to in-lab collections [5–7]. Employing machine learning models that use wearable sensors could overcome this limitation by providing mobile and real-time COM state estimates. Estimating the current state in time (i.e., zero-lag estimation) may not be the only possibility, as recent work has also shown that machine learning or other data-driven methods may enable estimates of future human states (i.e., anticipated estimation) [8–12]. These estimates could enable wearable robots that anticipate changes to human locomotion, rather than simply react to them.

However, COM state estimation during perturbed locomotion, the target for balance-augmenting wearable robots, is likely more challenging. These discrete and sudden changes to COM mechanics are likely more difficult for machine learning models to estimate, in comparison to steady state cyclic signals, because input sensor data windows may contain some pre-perturbation steady data and output labels are more transient, diverse, and may be less represented in the data set. Additionally, anticipated estimation compounds the challenge associated with this application, as wearable sensor input data will be less representative of perturbed mechanics. This is because machine learning models typically use some window of input sensor data to estimate a label; in anticipated estimation instances where the window ends right before the perturbation and the anticipated data point occurs shortly after the perturbation, it may be challenging for the model to accurately estimate this

point. However, recent advancements in human intent recognition using lower limb sensors are showing increased robustness across various modes of locomotion that suggest perturbed state estimation could be possible [13, 14].

Machine learning models using wearable sensors have shown significant promise in being able to estimate and predict human intent, especially from a reduced set of sensors [15, 16]. Specifically, deep learning models, such as temporal convolutional networks (TCN), have shown robustness in estimating continuous human states across various modes of locomotion [9, 13]. Previous work suggests that TCN models may outperform other deep learning methods, such as Long Short-Term Memory (LSTM) or Convolutional Neural Network (CNN) models, for wearable sensor-driven human state estimation [13]. The TCN architecture maintains the temporal order of input data and is relatively light-weight in terms of trainable parameters compared to a CNN. This reduced weight requires less data to sufficiently train the network, which is particularly appealing for human biomechanics applications in which data acquisition is time intensive. Thus, a TCN is a promising approach to investigate how well wearable sensor-informed data-driven models can estimate COM state during perturbed locomotion.

In this work, our broad goal was to investigate the ability of a wearable sensor-driven approach to estimate COM state during steady state and perturbed walking. We also evaluated how forward (anticipated) and backward (delayed) estimation influenced model accuracy, as anticipated estimation could enable more responsive exoskeleton controllers while delayed estimation could provide estimates with lower error at the expense of some delay [9]. To compare various exoskeleton sensor configurations, we simulated inertial measurement unit (IMU) sensors on the torso, pelvis, and lower limbs from a perturbed walking biomechanics data set. We quantified COM state as the mediolateral (ML) and anteroposterior (AP) COM position and velocity relative to the center of pressure (COP), shown in Fig. 1. First, we investigated the estimation capability of models that use only an inertial measurement unit (IMU) on the pelvis as well as sensor configurations that would be found on various lower limb robotic exoskeletons that combine multiple sensors. Next, we evaluated the delayed and anticipated estimation capability of a candidate exoskeleton sensor configuration. Lastly, we evaluated how various environmental perturbation conditions (magnitude, direction, and timing) influenced estimation accuracy. This work provides insight into the efficacy of COM estimation using wearable sensors for use in wearable robotic control during unstable locomotion.

## Materials and Methods

### Data Collection

All participants provided written informed consent for this study approved by the Georgia Institute of Technology Institutional Review Board. Eleven participants walked on a treadmill mounted in a six degree-of-freedom Stewart platform (CAREN, Motek Medical, Netherlands) [17]. Throughout the experiment, participants walked at 1.25 m/s. Participants were perturbed using surface translations that varied in magnitude (5, 10, 15 cm), direction (ML, AP, corresponding four diagonal combinations), and onset time (double stance; early, mid, late single stance), resulting in 96 unique conditions (Fig. 1). One perturbation occurred

approximately every 20 s, with the exact time being randomized to inhibit participant anticipation of the perturbation. The foot that the perturbation was applied on was also randomized to inhibit anticipation. Each participant walked for three sessions, resulting in three repetitions of each perturbation condition for a total of 288 perturbation trials per participant.

We collected a full-body marker set and five markers on the platform at 100 Hz, as well as bilateral ground reaction forces from the split-belt treadmill at 2000 Hz (Vicon, Oxford, United Kingdom). We collected readings from four tri-axial accelerometers (Model 4030, ± 2 G dynamic range, TE Connectivity, Switzerland) mounted on the Stewart platform at 2000 Hz for inertial compensation, which is discussed in the next section.

### Calculation of COM State Relative to COP

Due to the large inertia of the system, acceleration of the platform induced forces and moments on the force plates that needed to be corrected to obtain the forces and moments caused by the participant. We adapted and applied a previously published method that used platform-mounted accelerometers to identify and correct for induced forces and moments [18]. We used these corrected outputs to recalculate the COP and corrected the COP to accurately reflect the translation of the force plates with the platform relative to the global coordinate frame.

The motion capture marker data were lowpass filtered at 6 Hz using a fourth-order Butterworth filter. The COM was approximated by the mean of the four pelvis markers. We then calculated the ML and AP position and velocity relative to the combined COP from both force plates, providing continuous position and velocity measures throughout the gait cycle (Fig. 1). Across the 3168 collected perturbation trials, 27 resulted in a jump in response to the perturbation, defined by an aerial phase in the period after the perturbation onset. Because this results in a period of no center of pressure due to lack of ground contact, these trials were eliminated from the data set used in this work. The remaining 3141 perturbation trials were used in this analysis. The ML and AP position and velocity COM states were used as the data labels for the machine learning models.

### Inverse Kinematics and Simulated IMU Generation

From the collected biomechanics data set, we calculated simulated IMU sensor signals to represent the IMU set that would be found on a hip, knee, or ankle exoskeleton. We utilized simulated IMUs for this work because we did not have the ability to collect the entire set of physical IMUs required for this analysis. Utilizing simulated sensors allowed us to capitalize on this large and diversely perturbed data set while also allowing us to analyze a number of different sensor configurations that we believe would be informative for the wearable robotics and biomechanics communities. We calculated inverse kinematics using OpenSim 4.1 [19]. We used the OpenSim Scale Tool to scale a full-body musculoskeletal model to each participant [20]. We then used the OpenSim Inverse Kinematics Tool to obtain full-body joint kinematics. The resulting segment kinematics were then used to simulate linear acceleration and angular velocity recordings for mid-segment-mounted sensors on the

torso, pelvis, thigh, shank, and foot segments according to the protocol in [13]. This set of simulated IMUs was used as the inputs for the machine learning models.

### TCN Model Structure

We implemented a subject-independent TCN model that was previously found to outperform other deep learning models when estimating human outcomes during locomotion [13]. We altered the model to include a four-headed output to enable the estimation of ML and AP COM position and velocity with a single model. The model was split into four heads after the fully connected layer. All model hyperparameters were set as the optimal hyperparameters determined in [13], which investigated the capability of a comparable sensor set to estimate biomechanical outcomes during multimodal locomotion. The kernel size and levels hyperparameters dictate the required input data time history for a TCN model. The optimized hyperparameters in [13] require 187 points of time history, or 930 ms, based on the 200 Hz collection frequency used in the study.

### TCN Model Training and Testing Data

All collected perturbation trials, with the exception of the 27 eliminated trials discussed above, were used to provide the training and testing data for these analyses. All sensor and COM state data were upsampled from 100 to 200 Hz to replicate the collection frequency used in the study that provided the TCN hyperparameters used in this work [13]. For each perturbation trial, COM state labels were included for 2.95 s before and 6.05 s after the perturbation; this ensured the same labels were being estimated across delayed and anticipated estimation times, in which the sensor inputs window shifted relative to the COM state time point being estimated. We determined the across-participant mean steady state range of ML and AP position and velocity. These range values were 224 mm, 361 mm, 2956 mm/s, and 4126 mm/s for the ML position, AP position, ML velocity, and AP velocity, respectively. These across-participant means were used to scale all data labels, resulting in steady state signals with approximately the same range across all labels. These resulting labels are in units of percent of steady state range. We did this to prevent the multi-headed network from being biased toward outcome measures with larger ranges, and therefore larger error values for comparable error as a percentage of the steady state signal, during model training. Several perturbations in the data set regularly caused COM state deviations up to and surpassing 25% of the steady state range; thus, the model would need to achieve error values significantly below this to provide utility over a baseline approach of assuming steady state gait. We extracted input and label data for 50, 100, and 150 ms anticipated estimations (label was ahead in time from the last sensor input), 50, 100, and 150 ms delayed estimations (label was behind in time from the last sensor input), and zero-lag estimation (label was at same point in time as last sensor input, no delay or anticipation). Input data included all simulated IMUs and was 930 ms (or 187 data points) in length as discussed in the previous section. Label data included ML and AP COM position and velocity. Each TCN model was trained using 11-fold leave-one-subject-out validation using a mean squared error (MSE) loss function. Each model ran for 200 epochs, with a patience term of 50 epochs that enabled early stopping.

We trained and validated three sets of models. First, we trained a set of models to evaluate the performance of different wearable device sensor configurations for standard estimation. We evaluated configurations for pelvis only (pelvis IMU), hip exoskeleton (torso and thigh IMUs), knee exoskeleton (thigh and shank IMUs), ankle exoskeleton (shank and foot IMUs), and all sensors (torso, pelvis, thigh, shank, and foot IMUs). This resulted in 55 models being trained due to 11-fold leave-one-subject-out validation and 5 configuration conditions. Second, we trained a set of models using the hip exoskeleton sensor configuration for each of the delayed (50, 100, 150 ms) and anticipated (50, 100, 150 ms) estimation cases. This resulted in 66 more models being trained due to 11-fold leave-one-subject-out validation and 6 total delayed and anticipated estimation cases. Third, we trained and tested an additional set of models to investigate how well models trained on steady state and perturbed data were able to estimate steady state and perturbed COM states. Our primary goal was to investigate the importance of including perturbed data in the training set and what, if any, impact it would have on steady state and perturbed outcomes. To do this, we used a subset of the trials discussed above, producing two data sets; the steady state data set included 1 s of data before the perturbation for each trial, while the perturbed data set included 1 s of data after the perturbation for each trial. We then trained models using each data set using the same 11-fold leave-one-subject-out validation approach, testing both the steady state and perturbed data for each hold-out subject. This resulted in training 22 more models for this analysis. This resulted in training 143 total models for these analyses.

## Statistics

We performed statistical analyses using custom Matlab scripts (Mathworks, Natick, MA) and Minitab (Minitab 19, United States). For each trial, we evaluated the model performance on a steady state and perturbed subset of the data; we defined the steady state subset as the 1 s before the perturbation and defined the perturbed subset as the 1 s after perturbation. For both the steady state and perturbed subsets, we calculated the mean absolute error (MAE) and correlation strength ($R^2$) between the model's estimated and actual COM states. The mean of both MAE and $R^2$ were taken for every participant. All analyses were done on the participant means for every condition. To evaluate the effect of exoskeleton sensor configuration on mean absolute error (MAE) and correlation strength ($R^2$), we performed a oneway repeated measures ANOVA with sensor configuration as a fixed effect and participant as a random effect for each COM state outcome. We used post hoc comparisons with Bonferroni correction to evaluate sensor configuration comparisons. Resulting ANOVA $p$ values and significant comparisons are shown in Fig. 2. To evaluate the influence of estimation time, we again performed a one-way repeated measures ANOVA with estimation time as a fixed effect and participant as a random effect. We used post hoc comparisons with Bonferroni correction to evaluate the differences between zero-lag estimation and the six anticipated and delayed estimation times. Significant comparisons are shown in Fig. 3. To evaluate if perturbation conditions affected COM state estimates, we again used a one-way repeated measures ANOVA with perturbation condition as a fixed effect and participant as a random effect. We used post hoc comparisons with Bonferroni correction to evaluate the differences between perturbation conditions for groups with significant effects detected by the ANOVA. Resulting ANOVA $p$ values and significant comparisons are shown in Fig. 4. Lastly, to evaluate the influence of steady state and perturbed training data on various

outcomes, we performed a series of paired-sample $t$ tests. Significance between pairs is shown in Fig. 5. Across all analyses, the threshold for significance was set at $\alpha = 0.05$.

## Results

### Simulated Exoskeleton Sensor Configurations

We evaluated how various lower limb exoskeleton sensor configurations influenced MAE and $R^2$ of COM state estimates, with comparisons to baseline conditions that included a pelvis only IMU and all sensors (Fig. 2). During steady state walking, sensor configuration significantly affected MAE for all COM states except AP velocity and significantly affected $R^2$ for all COM state variables. During perturbed walking, sensor configuration significantly affected MAE and $R^2$ for all COM state outcomes. For perturbed ML position and velocity, the pelvis only MAE was higher than all other configurations, while the pelvis only $R^2$ was lower than the hip exoskeleton and knee exoskeleton configurations. For perturbed AP position, hip exoskeleton and all sensors configurations had significantly lower MAE than the other configurations; $R^2$ showed many differences between configurations, with the hip and all sensors configurations having the highest $R^2$. For perturbed AP velocity, the pelvis only MAE was higher than all other configurations, while the pelvis only $R^2$ was lower than all other configurations.

### Delayed and Anticipated Estimates

We evaluated the influence of estimation time on the MAE and $R^2$ of COM state estimates (Fig. 3). We aimed to determine if anticipated estimations (into the future) and delayed estimations (already occurred) significantly differed from zero-lag estimation. We evaluated the hip exoskeleton configuration as it showed the best performance of the lower limb exoskeletons evaluated in the across-configuration analysis. We chose to evaluate the hip exoskeleton configuration because the all sensors configuration did not provide significantly higher accuracy for any outcome and because it better represents a limited sensor set that would more feasible for implementation in wearable device or biomechanics experiments. During both steady state and perturbed walking, estimation time significantly affected MAE and $R^2$ for all COM state outcomes (all $p < 0.001$). During steady state walking, + 100 and + 150 ms (anticipated) estimates were significantly different from zero-lag estimation for all COM state variables for both MAE and $R^2$. The only significant differences detected for delayed estimates were for ML COM velocity MAE (− 100 and − 150 ms) and AP COM velocity MAE (− 150 ms). During perturbed walking, + 50, + 100, and + 150 ms (anticipated) estimates were significantly different from zero-lag estimates for all COM state variables for both MAE and $R^2$. For perturbed delayed estimates, significant differences were detected for ML COM position (− 150 for $R^2$), ML COM velocity (− 100 and − 150 ms for both MAE and $R^2$), and AP COM velocity (− 50, − 100, and − 150 ms for MAE and $R^2$).

### Influence of Perturbation Conditions

We evaluated the influence of perturbation magnitude, direction, and timing on MAE of zero-lag COM estimation (no delay or anticipation time; Fig. 4). We again evaluated the hip exoskeleton sensor configuration. Perturbation magnitude significantly affected all COM

state estimates, with MAE increasing with increased perturbation magnitude. We detected significant differences between all perturbation magnitude conditions for all outcomes except between small (5 cm) and medium (10 cm) as well as medium (10 cm) and large (15 cm) perturbations for the ML position estimates. However, perturbation direction only affected ML and AP velocity estimates, with lateral (shown in pink) and anterolateral perturbations (shown in red) typically causing the highest MAE. Anterior and posterior perturbations (shown in orange and blue, respectively) tended to cause the lowest error across COM state outcomes. We only detected significant differences between individual conditions for the ML velocity estimates; we detected differences between the lateral (pink)/anterior (orange), lateral (pink)/posterior (blue), anterolateral (red)/anterior (orange), and anterolateral (red)/posterior (blue) conditions. Representative trials for the purely AP and ML perturbations are shown in Fig. 6. Lastly, perturbation timing did not significantly affect any of the COM state estimates.

### Influence of Training Data Type

We evaluated the influence of steady state and perturbed training data on steady state and perturbed estimation outcomes (Fig. 5). We aimed to investigate how models trained on different types of data (steady state, perturbed) would influence the accuracy of COM estimates. We evaluated zero-lag estimation outcomes using the hip exoskeleton configuration as it showed the best performance of the lower limb exoskeletons evaluated in the across-configuration analysis. The steady state COM state estimate MAE values were not significantly affected by the training data types. However, the $R^2$ value for the AP position estimates was significantly higher for the steady state-trained model in comparison to the perturbed-trained model. The perturbed COM state estimate MAE and $R^2$ values between steady state-trained models and perturbed-trained models were significant for all COM state outcomes.

## Discussion

### Exoskeleton Sensor Configurations

The first question that we aimed to investigate in this work was how well various lower limb exoskeletons could estimate COM state given a standard IMU sensor set on each device. To provide baseline comparisons, we also evaluated the performance of a single simulated pelvis IMU, which is on the same segment used to approximate COM from biomechanical data, as well as all sensors. We found that the pelvis sensor performed significantly worse than the other exoskeleton configurations, primarily when estimating COM state during perturbed walking (Fig. 2). This indicates that a single sensor is likely not sufficient for COM state estimation but using segment-mounted sensors on a single joint exoskeleton is sufficient to maximize accuracy. Interestingly, we found few significant differences between exoskeleton sensor configurations. This finding includes the comparison to the all sensors configuration, indicating that increasing the number of sensors, relative to the three or four sensors on single joint exoskeletons, does not further improve predictions. This indicates that various lower limb exoskeletons could provide accurate COM estimates without the need for additional sensors, enhancing the efficacy of this approach. Because the hip exoskeleton sensor set outperformed the pelvis more than the other exoskeleton

configurations, we evaluated the hip exoskeleton configuration for the remainder of the analysis.

## Delayed and Anticipated Estimates

We also wanted to evaluate how anticipated and delayed estimation times affected accuracy and correlation strength relative to zero-lag estimation (Fig. 3). Across all COM state estimates, steady state estimates were more accurate than perturbed. Because perturbations abruptly and transiently disrupt a usually cyclic COM state, we expected that the model would estimate perturbed COM state with lower accuracy. Across all COM state estimates, greater anticipation times decreased accuracy. This is the expected result, as predicting future CoM state changes during perturbed locomotion becomes highly challenging due to the lack of relevant time history information. However, the anticipated estimates are still promising, as the error for even the 150 ms anticipated estimates did not even double the error of zero-lag (0 ms) estimates. Greater anticipation times are possible, but will likely cause increasing error and poorer performance, specifically immediately following the perturbation onset. These anticipated estimates could be used to enable faster exoskeleton responses, due to the system anticipating the user's state rather than simply reacting to it. We expected better performance for delayed estimates, as the input data span the point in time that the estimate is being made for (i.e., the sensors include data from before and after the desired COM state estimate) [9]. Our results suggest that this is the case, with delayed estimates improving accuracy relative to zero-lag estimates across multiple COM state outcomes, particularly for COM velocity estimates. However, greater delay times (up to or exceeding 150 ms) may not be necessary to achieve this bump in accuracy, as there is relatively little difference in error across 50, 100, and 150 ms delays. The more accurate delayed estimates could be employed to enable mobile data collection, update machine learning models in real time to customize models to individual users, or in applications where a small amount of delay is acceptable.

## Influence of Perturbation Conditions

We also investigated how different perturbation characteristics affected COM state estimation error (Fig. 4). First, perturbation magnitude had a clear effect on error, with increased perturbation magnitude causing increased error across all COM state variables. Additionally, perturbation direction significantly affected COM velocity error, but not position error; lateral and anterolateral perturbations, which induce a widening step maneuver, caused the most error across all COM state outcomes. Previous work has shown comparable trends in how balance is influenced by these perturbation conditions [17, 21]. This may suggest that error simply scales with the magnitude of the COM state signal, as higher magnitude perturbations and lateral perturbations have been shown to cause greater deviations in balance metrics and human recovery strategies. Lastly, we found that perturbation onset timing during the gait cycle did not significantly affect error for any COM state estimate. This suggests that this approach could be viable when deployed in uncontrolled environments where perturbations can onset at any time. The thoroughly significant effect of perturbation magnitude but not necessarily direction or timing is possibly caused by the represented data in the training set. Generally, machine learning models are better at interpolating than extrapolating. Both the direction and timing variables

are uniformly sampled from a “cyclic” or “circular” space in which all possible direction or timing conditions are reasonably captured by the training data. However, perturbation magnitude exists in a linear space where larger perturbations are near the bounds of the data represented in the training set, likely causing higher estimation errors for those conditions.

### Influence of Training Data Type

We aimed to investigate the importance of including perturbed data in the training set. We predicted that including perturbed data in the training set would be necessary to reduce error in perturbed estimates, with steady state-trained models providing poor estimates of perturbed outcomes. However, we also predicted that perturbation-trained models would slightly reduce the accuracy of steady state estimates in comparison to models that were trained only on steady state data. We found that, largely, training models with perturbed data did not reduce the accuracy of steady state estimates. However, we also found that including perturbed data in the training set is crucial to improve the accuracy of perturbed COM state estimates. Broadly, this work implies that you may not need to choose between accurate steady state and perturbed estimates. Rather, expanding training sets to include diversely perturbed locomotion enhances perturbed estimates without sacrificing steady state accuracy.

### Broader Implications, Limitations, and Future Directions

This work has shown that estimating COM state using sensors typically onboard a single joint lower limb robotic exoskeleton is feasible. Specifically, the comparable performance of sensor sets for hip and ankle exoskeletons is a promising sign for balance-augmenting exoskeleton research. Previous work in this area has focused on hip and ankle exoskeletons due to the role of these joints in generating balance-correcting responses [5–7, 22, 23]. Our approach to estimate COM state could be deployed on hip or ankle exoskeleton devices to enable exoskeleton controllers that correct for COM changes following perturbations. Additionally, this work demonstrates the ability of machine learning approaches to generate anticipated estimates that could enable wearable robots to be proactive rather than reactive by using future COM states to drive control. Our findings suggest that it is crucial to train models using perturbation conditions or other destabilizing conditions that are representative of the desired use case, and that doing so will not sacrifice steady state estimation accuracy.

This work also has limitations that should be considered by researchers looking to build off of these findings. First, the use of simulated IMUs assumes perfect coupling between the sensors and the participant’s skeleton. When implemented with physical sensors, soft tissue noise and decoupling between the user and exoskeleton, especially during periods of high torque assistance, could affect the IMU data. These challenges could be mitigated by layering noise profiles onto simulated IMU data for more representative training data, using high-fidelity IMUs that present cleaner signals than IMUs more traditionally used in wearable robotic applications, or placing IMUs directly on the user rather than on the device to minimize user-exoskeleton decoupling during torque assistance. Additionally, the user’s COM was approximated in this work using the average of four pelvis-mounted motion capture markers. Depending on the use case of this model, this could be altered to better approximate the whole-body COM by considering the combined COM of all body

segments. Another important limitation to note is that this work was performed on a fixed speed instrumented treadmill. Though the perturbation platform and treadmill provide an opportunity for repeatable and controlled perturbations to study, the fixed speed and lateral boundaries of the treadmill also limit the participants' natural response. Future studies could build off of this work by training and testing COM estimation models in unconstrained overground environments.

Though simulated IMUs are one of the limitations of this work, our approach mitigates some of the shortcomings that IMUs often present for position-based estimation. IMUs are typically sensors that introduce issues such as noise and drift over time, with drift becoming increasingly problematic for position-based estimates that require single or double integration of the native gyroscope and accelerometer signals (e.g., dead reckoning). This emphasizes a key benefit of machine learning-based approaches, which do not utilize integration and thus do not experience any drift. Our approach creates a mapping between the previous 930 ms of accelerometer and gyroscope data and the COM state, rather than directly integrating signals over time, to attain a position estimate which avoids issues associated with sensor drift. However, these IMUs still only provide kinematic information and are likely far less reflective of COP changes underneath the foot. Though the approach presented in this work is promising, additional sensing could further enhance COM state estimation accuracy. The use of pressure insoles, which typically measure the vertical force and the ML and AP COP underneath the foot, would likely further enhance this approach. This addition could be particularly helpful in better estimating the sudden COM state changes immediately following perturbations or other transient, rapid changes to the COM.

The work presented here utilizes previously optimized TCN hyperparameters from [13]. Because the estimation, and especially anticipated estimation, of biomechanical outcomes during unsteady locomotion is a relatively nascent area of research, there are many possible avenues that could expand on the results presented here. First, further tuning the TCN's hyperparameters could assist in bettering tailoring the model to perturbed applications. Specifically, there are opportunities to explore how input data time history should be tailored for perturbed applications, where longer time histories that have utility during steady state locomotion may not be as relevant to estimate rapid, transient changes in biomechanical outcomes. However, due to the structure of a TCN, increased time history also correlates with increased model depth that may enhance the model's ability to learn from the training data. Thus, there are opportunities for hyperparameter tuning, as well as the exploration of different or hybrid structures that optimize model structures for perturbed locomotion [24, 25]. Further model alterations and tuning could also be beneficial depending on the eventual use case of such a model. If used for perturbation detection, researchers may want to optimize the model's performance in the immediate time windows after the perturbation. If used for continuous exoskeleton control, researchers may need to consider max error in addition to MAE to smooth out continuous model performance, as well as constrain exoskeleton output torques to mitigate transient model errors. If used for intermittent exoskeleton control, researchers could modify testing data sets to isolate model tuning and performance evaluation to the exact targeted use cases. Broadly, this work provides strong initial support for the feasibility of real-time COM state estimates for exoskeleton control and opens many avenues for further refining these models for various use cases.

In future applications, the COM state estimation models in this work could be used to develop intelligent exoskeleton control architectures that react to COM state changes using concepts such as capture point and extrapolated center of mass to drive step placement, ankle moment modulation, or other balance-correcting responses [1, 2, 5, 26]. Other applications of this work could be collecting COM state data outside of a traditional biomechanics lab or using COM state for biofeedback in balance rehabilitation applications. Broadly, this work demonstrates that COM state estimation is possible with reduced sensor sets, for different delayed and anticipated estimation times, and across a large diversity of perturbation conditions.

## Acknowledgments

The authors would like to thank Z. Centeno Sanz and V. Iyer for their help building the code for COP correction, P. Golyski and D. Espinal for their help with data collection, D. Molinaro for providing guidance on the TCN model, and E. Schonhaut for his assistance running models. This work was supported by National Science Foundation Research Traineeship: Accessibility, Rehabilitation, and Movement Science (NSF NRT ARMS) Program Award #1545287, National Science Foundation Graduate Research Fellowship Program (NSF GRFP) Award #1324585, the Georgia Institute of Technology Petit Institute Pruitt Scholarship, and NIH Director's New Innovator Award DP2-HD111709.

## References

1. Pratt J, Carff J, Drakunov S, and Goswami A. Capture point: a step toward humanoid push recovery. In: 2006 6th IEEE-RAS International Conference on Humanoid Robots. University of Genova, Genova, Italy. IEEE, 2006, pp. 200–207. 10.1109/ICHR.2006.321385.
2. Hof AL The 'extrapolated center of mass' concept suggests a simple control of balance in walking. Hum. Mov. Sci 27(1):112–125, 2008. 10.1016/j.humov.2007.08.003. [PubMed: 17935808]
3. Wang Y, and Srinivasan M. Stepping in the direction of the fall: the next foot placement can be predicted from current upper body state in steady-state walking. Biol. Lett 10(9):20140405, 2014. 10.1098/rsbl.2014.0405. [PubMed: 25252834]
4. Simonetti E, Bergamini E, Vannozzi G, Bascou J, and Pillet H. Estimation of 3D body center of mass acceleration and instantaneous velocity from a wearable inertial sensor network in transfemoral amputee gait: a case study. Sensors. 21(9):Art. no. 9, 2021. 10.3390/s21093129.
5. Zhang T, Tran M, and Huang H. Design and experimental verification of hip exoskeleton with balance capacities for walking assistance. IEEE/ASME Trans. Mechatron 23(1):274—285, 2018. 10.1109/TMECH.2018.2790358.
6. Afschrift M, et al. Assisting walking balance using a bio-inspired exoskeleton controller. J. Neuroeng. Rehabil 20:82, 2023. 10.1186/s12984-023-01205-9. [PubMed: 37370175]
7. Bayón C, Keemink AQL, van Mierlo M, Rampeltshammer W, van der Kooij H, and van Asseldonk EHF. Cooperative ankle-exoskeleton control can reduce effort to recover balance after unexpected disturbances during walking. J. NeuroEng. Rehabil 19(1):21, 2022. 10.1186/s12984-022-01000-y. [PubMed: 35172846]
8. Camargo J, Molinaro DD, and Young AJ. Predicting biological joint moment during multiple ambulation tasks. J. Biomech 134:111020, 2022. 10.1016/j.jbiomech.2022.111020. [PubMed: 35228154]
9. Molinaro DD, Park EO, and Young AJ. Anticipation and delayed estimation of human hip moments using deep learning and a robotic hip exoskeleton. IEEE ICRA. 2023.
10. Hollinger D, Schall M, Chen H, Bass S, and Zabala M. The influence of gait phase on predicting lower-limb joint angles. IEEE Trans. Med. Robot. Bionics 5(2):343–352, 2023. 10.1109/TMRB.2023.3260261.
11. Lee S-W, and Asbeck A. A deep learning-based approach for foot placement prediction. IEEE Robot. Autom. Lett 8(8):4959–4966, 2023. 10.1109/LRA.2023.3290521.

12. Tanghe K, De Groote F, Lefeber D, De Schutter J, and Aertbeliën E. Gait trajectory and event prediction from state estimation for exoskeletons during gait. IEEE Trans. Neural Syst. Rehabil. Eng 28(1):211–220, 2020. 10.1109/TNSRE.2019.2950309. [PubMed: 31675336]
13. Molinaro DD, Kang I, Camargo J, Gombolay MC, and Young AJ. Subject-independent, biological hip moment estimation during multimodal overground ambulation using deep learning. IEEE Trans. Med. Robot. Bionics 4(1):219–229, 2022. 10.1109/TMRB.2022.3144025.
14. Dorschky E, Nitschke M, Martindale CF, van den Bogert AJ, Koelewijn AD, and Eskofier BM. CNN-based estimation of sagittal plane walking and running biomechanics from measured and simulated inertial sensor data. Front. Bioeng. Biotechnol 8:604, 2020. 10.3389/fbioe.2020.00604. [PubMed: 32671032]
15. Lim H, Kim B, and Park S. Prediction of lower limb kinetics and kinematics during walking by a single IMU on the lower back using machine learning. Sensors. 20(1):130, 2020. 10.3390/s20010130.
16. Camargo J, Flanagan W, Csomay-Shanklin N, Kanwar B, and Young A. A machine learning strategy for locomotion classification and parameter estimation using fusion of wearable sensors. IEEE Trans. Biomed. Eng 68(5):1569—1578, 2021. 10.1109/TBME.2021.3065809. [PubMed: 33710951]
17. Leestma JK, Golyski PR, Smith CR, Sawicki GS, and Young AJ. Linking whole-body angular momentum and step placement during perturbed walking. J. Exp. Biol 226(6):jeb244760, 2023. 10.1242/jeb.244760. [PubMed: 36752161]
18. Hnat SK, van Basten BJH, and van den Bogert AJ. Compensation for inertial and gravity effects in a moving force platform. J. Biomech 75:96–101, 2018. 10.1016/j.jbiomech.2018.05.009. [PubMed: 29789150]
19. Delp SL, et al. OpenSim: open-source software to create and analyze dynamic simulations of movement. IEEE Trans. Biomed. Eng 54(11):1940–1950, 2007. 10.1109/TBME.2007.901024. [PubMed: 18018689]
20. Rajagopal A, Dembia CL, DeMers MS, Delp DD, Hicks JL, and Delp SL. Full-body musculoskeletal model for muscle-driven simulation of human gait. IEEE Trans. Biomed. Eng 63(10):2068–2079, 2016. 10.1109/TBME.2016.2586891. [PubMed: 27392337]
21. Vlutters M, Van Asseldonk EHF, and Van der Kooij H. Center of mass velocity based predictions in balance recovery following pelvis perturbations during human walking. J. Exp. Biol 219(10):1514–1523, 2016. 10.1242/jeb.129338. [PubMed: 26994171]
22. Chiu VL, Raitor M, and Collins SH. Design of a hip exoskeleton with actuation in frontal and sagittal planes. IEEE Trans. Med. Robot. Bionics 3(3):773–782, 2021. 10.1109/TMRB.2021.3088521.
23. Alili A, Fleming A, Nalam V, Liu M, Dean J, and Huang H. Abduction/adduction assistance from powered hip exoskeleton enables modulation of user step width during walking. IEEE Trans. Biomed. Eng 71(1):334–342, 2023. 10.1109/TBME.2023.3301444. [PubMed: 37540615]
24. Liang W, Wang F, Fan A, Zhao W, Yao W, and Yang P. Deep learning model for the prediction of lower-limb joint moments using single inertial measurement unit during different locomotive activities. Biomed. Signal Process. Control 86:105372, 2023. 10.1016/j.bspc.2023.105372.
25. Hossain MSB, Guo Z, and Choi H. Estimation of lower extremity joint moments and 3D ground reaction forces using IMU sensors in multiple walking conditions: a deep learning approach. IEEE J. Biomed. Health Inform 27(6):2829–2840, 2023. 10.1109/JBHI.2023.3262164. [PubMed: 37030855]
26. Reimann H, Fettrow TD, Thompson ED, Agada P, McFadyen BJ, and Jeka JJ. Complementary mechanisms for upright balance during walking. PLoS ONE 12(2):e0172215, 2017. 10.1371/journal.pone.0172215. [PubMed: 28234936]

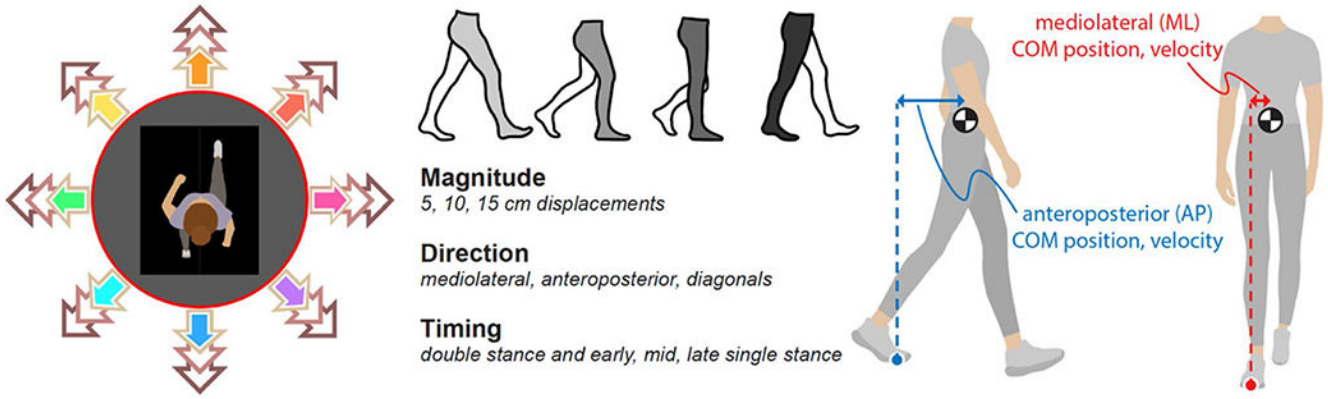


**Fig. 1.**

Perturbations varied in magnitude (left, shown by colored arrows), direction (left, shown by colored arrow outlines), and timing (top walking diagram). Center of mass (COM) state was defined using the mediolateral (ML) and anteroposterior (AP) position and velocity vectors between the COM and continuous center of pressure (COP) spanning both feet, representing the COM in a local reference frame defined by the point of ground contact

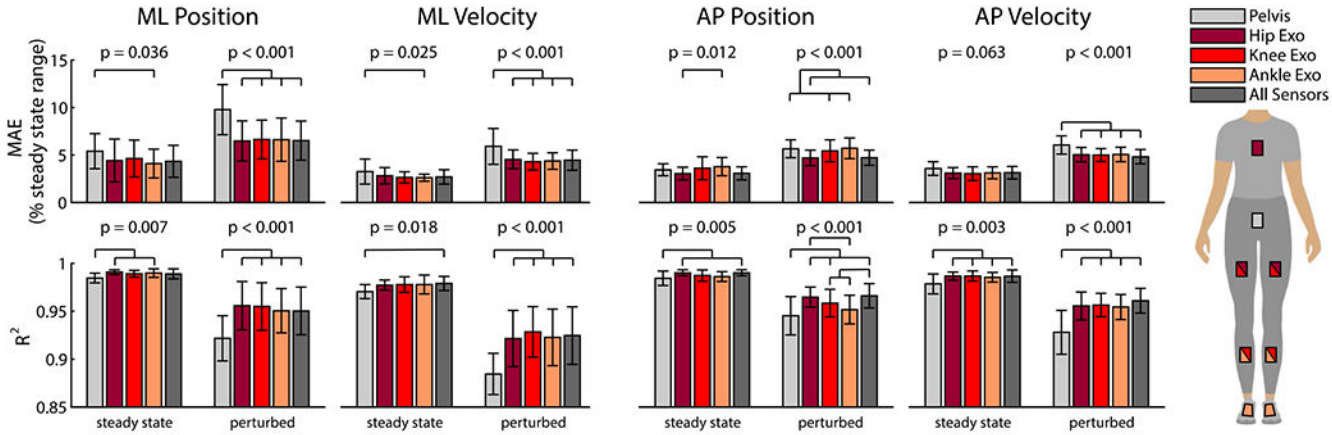


**Fig. 2.**

The effect of exoskeleton sensor configuration on mean absolute error (MAE, lower is better) and $R^2$ (higher is better) for center of mass (COM) state estimation. MAE and $R^2$ are shown for mediolateral (ML) and anteroposterior (AP) position and velocity estimates during both steady state (1 s before perturbation) and perturbed (1 s after perturbation) estimates. These values were calculated from the across-trial means for each participant, causing 11 samples to make up each distribution. The bars and error bars show the across-participant mean and ± 1 standard deviation, respectively. Results are shown for zero-lag estimation, not delayed or anticipated estimation. For each subplot, the $p$ value shows the results of a one-way repeated measures ANOVA and the comparison bars indicate significant differences detected between exoskeleton sensor configurations. For both, the threshold for significance was set at $\alpha = 0.05$

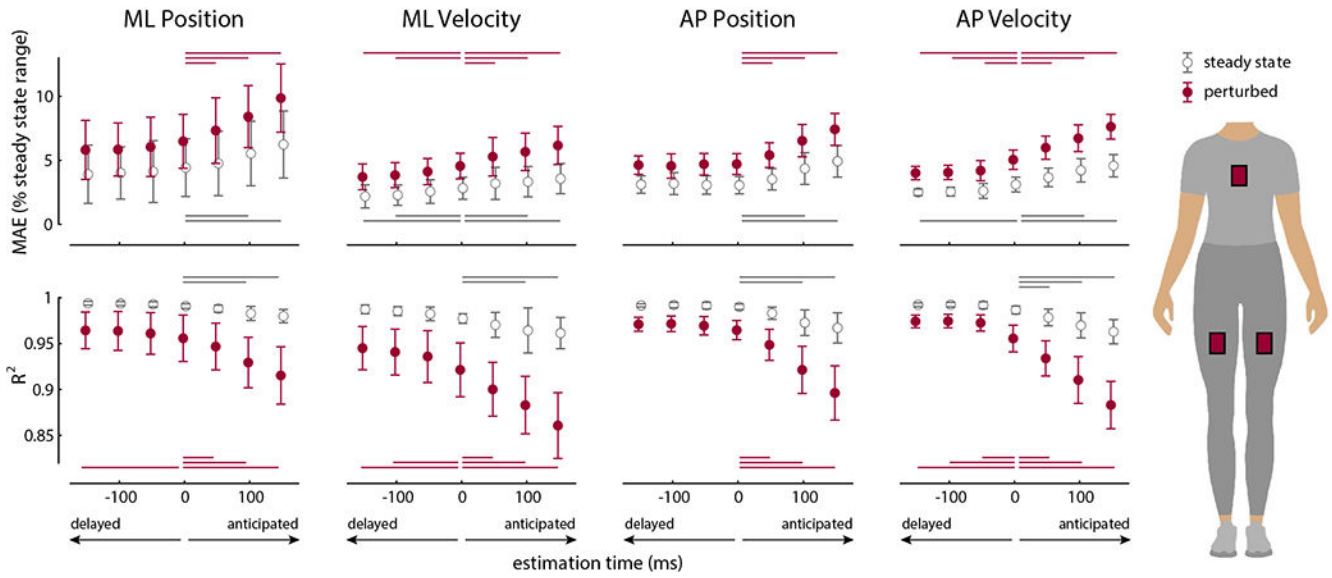


**Fig. 3.**

The effect of estimation time on mean absolute error (MAE, lower is better) and $R^2$ (higher is better) for center of mass (COM) state estimation. MAE and $R^2$ are shown for mediolateral (ML) and anteroposterior (AP) position and velocity estimates during both steady state (1 s before perturbation, shown in gray) and perturbed (1 s after perturbation, shown in red) COM state estimates. These values were calculated from the across-trial means for each participant, causing 11 samples to make up each distribution. The circular markers and error bars show the across-participant mean and ± 1 standard deviation, respectively. Slight offsets were used along the x-axis for better clarity of overlapping standard deviation bars and do not reflect different estimation times between the steady state and perturbed models. All results are shown for the hip exoskeleton sensor configuration (right). Comparison bars indicate significant differences detected between zero-lag (0 ms) estimation and other estimation times. The threshold for significance was set at $\alpha = 0.05$

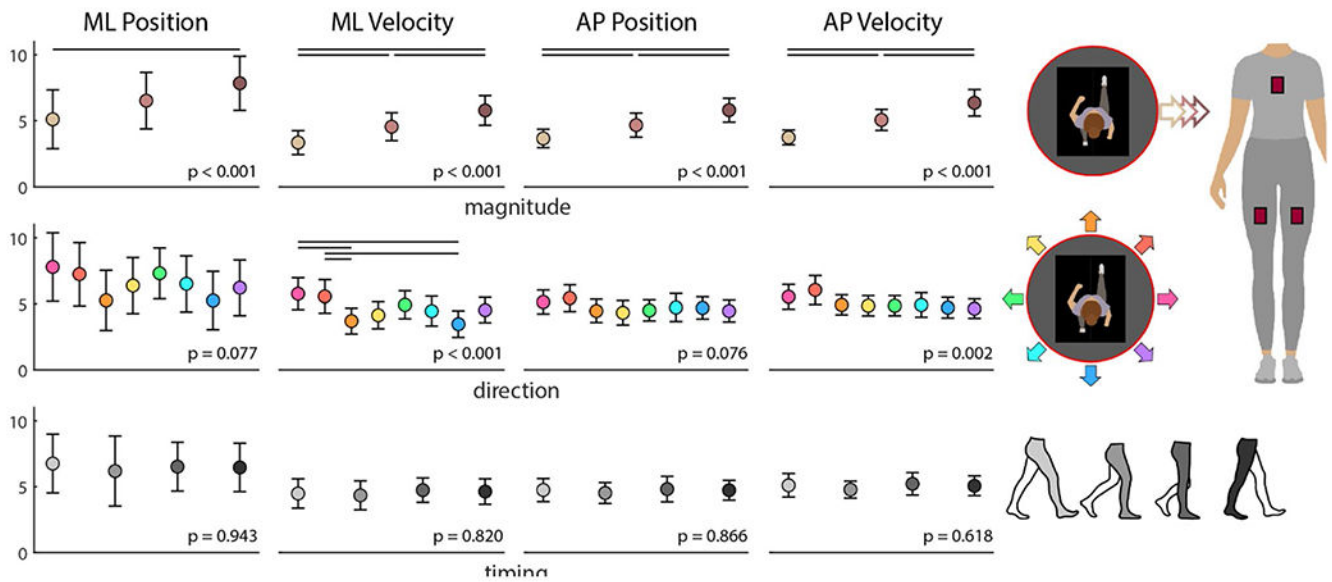


**Fig. 4.**

The effect of perturbation conditions on mean absolute error (MAE, lower is better) for perturbed center of mass (COM) state estimation. MAE is shown for mediolateral (ML) and anteroposterior (AP) position and velocity estimates. The rows show the effect of magnitude, direction, and timing, with the colored diagrams (right) illustrating the represented conditions. These values were calculated from the across-trial means for each participant, causing 11 samples to make up each distribution. The circular markers and error bars show the across-participant mean and ± 1 standard deviation, respectively. All results are shown for the hip exoskeleton sensor configuration (right) for zero-lag estimation. For each subplot, the $p$ value shows the result of a one-way repeated measures ANOVA. Comparison bars indicate significant differences detected between conditions. The threshold for significance was set at $\alpha = 0.05$

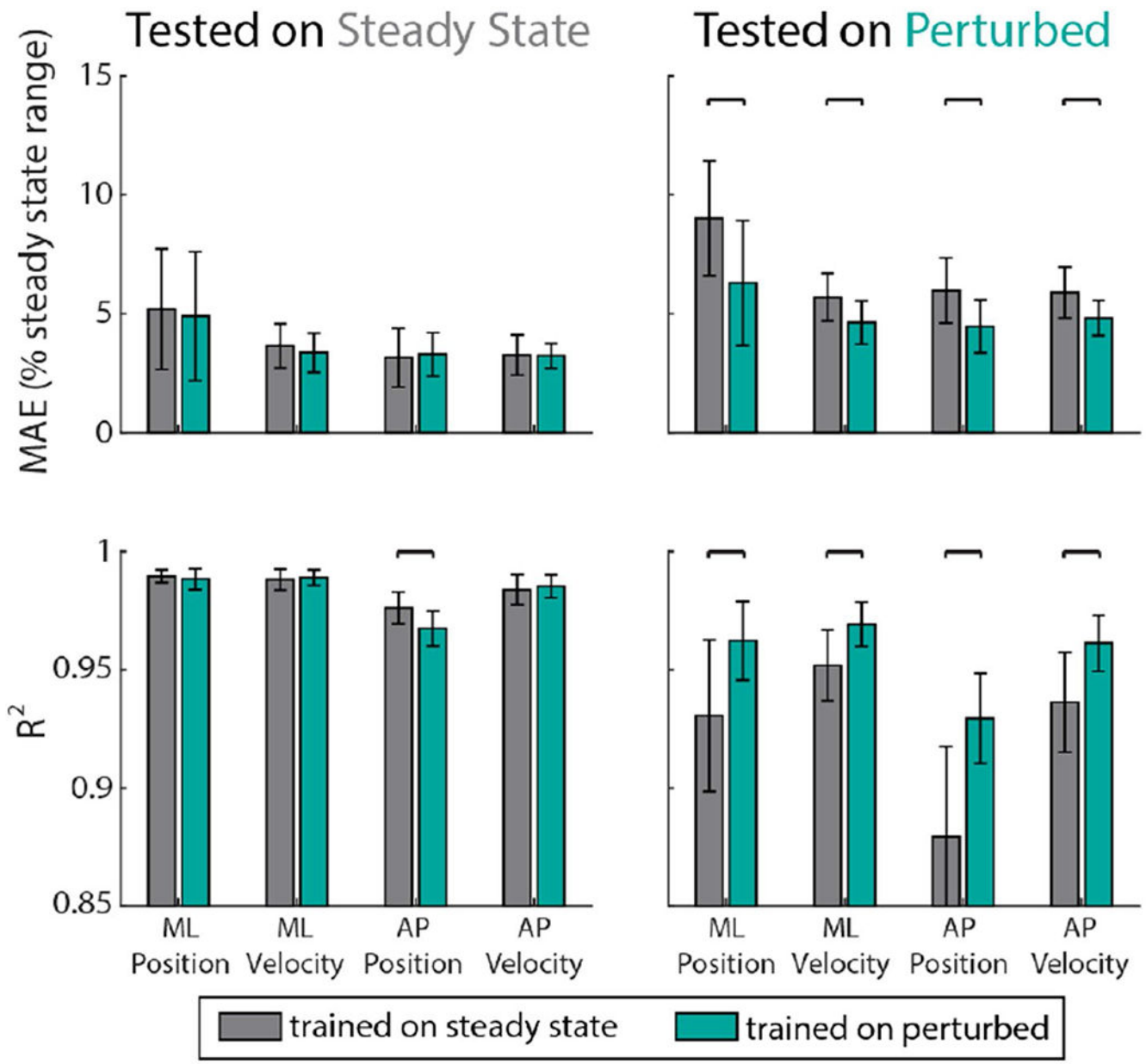


**Fig. 5.**

The effect of steady state and perturbed training data on mean absolute error (MAE, lower is better) and $R^2$ (higher is better) for steady state and perturbed center of mass (COM) state estimation. MAE and $R^2$ are shown for mediolateral (ML) and anteroposterior (AP) position and velocity estimates. These values were calculated from the across-trial means for each participant, meaning 11 samples make up each distribution. The bars and error bars show the across-participant mean and ± 1 standard deviation, respectively. All results are shown for the hip exoskeleton sensor configuration for zero-lag estimation. Comparison bars indicate significant differences detected between models that were trained on steady state and perturbed data. The threshold for significance was set at $\alpha = 0.05$

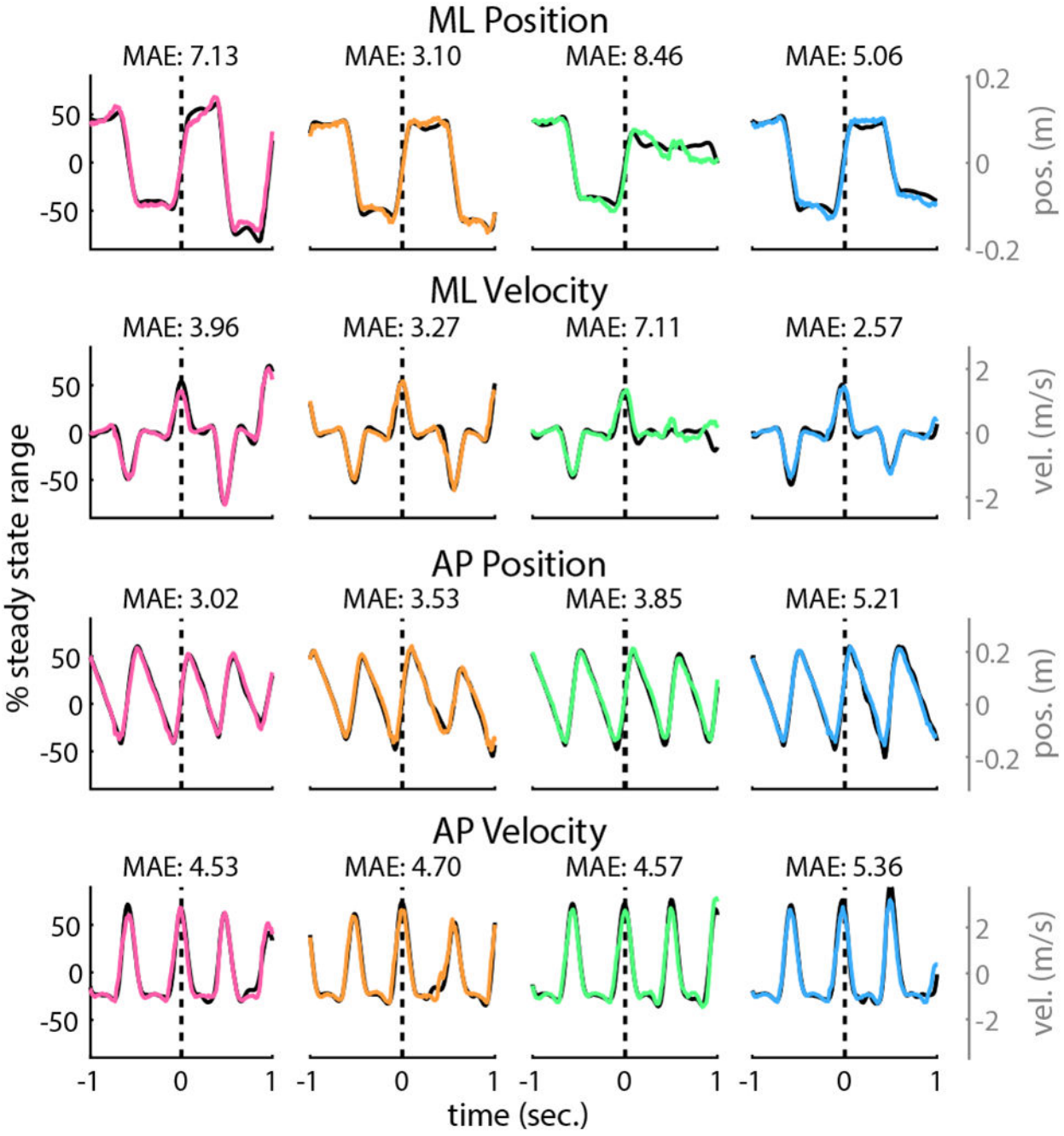


**Fig. 6.**

Representative labels (black) and estimates (colors) for a single trial across four perturbation directions; lateral (pink), anterior (orange), medial (green), and posterior (blue) perturbations are shown in columns one through four, respectively. Results are shown for mediolateral (ML) and anteroposterior (AP) position and velocity estimates. The perturbation is represented by the dashed line, where the left side is steady state data and the right side is the second following perturbation onset. All trials shown above were for a 10 cm perturbation and double stance onset time. The mean absolute error (MAE) shown for each

subplot indicates perturbed COM state MAE (after 0 s. on *x*-axis). The left and right *y*-axes show normalized and unnormalized units, respectively